Mechanistic Design Considerations for Punchout Distress in Continuously Reinforced Concrete Pavement

DAN G. ZOLLINGER AND ERNEST J. BARENBERG

A study was undertaken at the University of Illinois to develop a mechanistic design approach for continuously reinforced concrete (CRC) pavements to account for punchout distress. A mechanism relating to the loss of load transfer and the progressive development of punchout-related distress is presented. Analysis procedures, demonstrated to implement the mechanism as a rationally based thickness design procedure for CRC pavement, suggest that the optimal crack interval is between 3 and 4 ft. Present CRC design methodologies focus on limiting to certain design criteria cracking intervals, crack width, and stress in the reinforcements. Load transfer mechanisms have not been considered in the limiting design criteria and consequently are not included in these design procedures. These methods attempted to determine the design pavement thickness based on the combined effects of environmental and load-related stress on the final crack spacing, which must be limited to the design cracking criteria. However, past experience has indicated that a certain percentage of crack spacing usually falls below the specified minimum crack interval. These data suggest a greater tendency for punchouts to develop within this lower range of crack spacing. How pavement thickness, percent reinforcement, and crack spacing may be considered with respect to pavement spalling and loss of load transfer in the process of punchout development are outlined.

Continuously reinforced concrete (CRC) pavements exhibit distinctive cracking patterns induced by the restraint to volumetric strains in the concrete material caused by the reinforcing steel. This type of pavement, in which the longitudinal reinforcement is placed in a continuous configuration, can be considered as an alternative to jointed concrete pavement in some instances. Once the transverse cracks develop, the role of the reinforcement is to maintain the crack width below certain levels so that, in combination with the pavement thickness, a high degree of load transfer efficiency can be achieved throughout the design life. The primary pavement distress in CRC pavements is the punchout and faulting between closely spaced transverse cracks. This distress is a manifestation of the loss of load transfer across the transverse cracks. Therefore, there is evident need for thickness design analysis of CRC pavement based on punchout failure mechanisms to improve the reliability against premature punchout development.

D. G. Zollinger, Department of Civil Engineering and Texas Transportation Institute, Texas A&M University, College Station, Tex. 77843. E. J. Barenberg, Department of Civil Engineering, University of Illinois, Urbana-Champaign, Ill. 61801.

Present thickness design procedures for CRC pavements are either based on a thickness ratio between CRC pavement and jointed concrete design thickness (*1*,*2*) or are indirectly related to limiting design criteria for calculated structural response parameters (*3*), or both. Neither of these methods for selection of the design thickness of CRC pavement considers load transfer across the transverse cracks directly. The latter method, which has been adopted into the 1986 AASHTO Design Guide (*3*) and into the Concrete Reinforcing Steel Institute (CRSI) design manual (*4*) for CRC pavement, approaches the design of CRC pavements by focusing on the prediction of crack spacing, crack width, and steel stress as a function of wheel load and environmentally induced contraction. The design crack width and steel stress are dependent on the design crack spacing, which is a function of the percentage of reinforcement and wheel load stress. Therefore, the percentage of reinforcement (and the wheel load stress as input) is determined so that the limiting design criterion applied to crack spacing, crack width, and steel stress indirectly produces a design pavement thickness. The design thickness is derived from this procedure because the percent of reinforcement and the wheel load stress are a function of the pavement thickness.

Present procedures recommend that crack spacing should be selected so that the crack width is small enough to minimize the entrance of surface water and to provide the necessary load transfer through aggregate interlock (*5*). The cracking design criteria have evolved over time to include shorter cracking intervals. Intervals initially were set between 5 and 8 ft based on deflection test results and steel corrosion studies (*6*). Most recently minimum crack spacing has changed to as low as 3 ft based on an arbitrary load transfer and pavement stiffness relationship. Field performance has suggested that the maximum crack spacing is a function of pavement spalling and should range between 6 and 8 ft (*7*). Frequently, punchout distress shows up in pavement sections with crack spacing of 1 to 2 ft. In spite of the limiting design criteria, a certain percentage of crack spacing usually falls below the specified minimum crack interval. A short cracking interval has been recognized as an undesirable feature (*6*).

Correlations between CRC pavement thickness and jointed pavement thickness are taken from present serviceability index ratings for jointed concrete pavement. The thickness design of jointed pavements was derived from performance equations developed from the AASHO Road Test predicting the future serviceability as a function of equivalent 18-kip single-axle load applications. These methods usually have resulted

in thicknesses less than that for jointed concrete pavement. Reported correlations were also made based on deflections comparisons (*8*) made in Texas, but they were not as conclusive. The 1986 AASHTO Design Guide describes thickness design for jointed and continuously reinforced concrete pavements by the same performance equations, meaning no reduction in CRC thickness. These equations consider the traffic level, concrete strength, modulus of support (K value), load transfer, terminal serviceability index, and design reliability. Load transfer is characterized by a load transfer coefficient (J), which is recommended in terms of the shoulder type. Tied concrete shoulders allow for lower J factors, which leads to less thickness. The J factor ranges from 2.9 to 3.2 for an asphalt shoulder to 2.3 to 2.9 for a tied concrete shoulder. Justification for the J factor has been somewhat subjective in past design guides (*9,10*) and still is to a certain extent, inasmuch as it is based on experience and mechanistic stress analysis (*3*). The applicability of equations and relationships describing the performance of jointed concrete pavements to CRC pavements has never been verified. Many state thickness standards have established 8 in. as a minimum CRC pavement thickness. However, the trend has been toward greater CRC pavement thicknesses since reports have been favorable of 10-in. CRC pavements under heavy traffic loads (*11*). Current design practice in which yielding pavement thicknesses are too thin has been under suspicion (*12*).

Several early failures have been attributed to excessive deflections under heavy loads, suggesting that greater thicknesses will improve performance. A move toward greater design thicknesses for CRC pavements is likely to be beneficial for performance. It appears, however, that the recommended increase in thickness is arbitrarily determined in the most recent version of the AASHTO Design Guide, i.e., there appears to be no well-defined, rational method to determine the thickness of CRC pavement. Since punchouts are the primary structural type of distress in CRC pavements, there is a need to understand punchout distress mechanisms and how they relate to thickness design and pavement performance to establish a basis for mechanistic thickness design. Arguments for increased CRC design thicknesses are difficult to justify unless punchout-related mechanisms are incorporated into the design procedure. Given the uncertain performance of CRC pavement, there is little doubt that thickness design must address more directly the variables that influence punchout performance (*12*).

Recently developed mechanistic analysis (*13–15*) models have established markedly different types of structural behavior between jointed and CRC pavements. Consequently, consideration for load and support conditions different from those of the AASHO Road Test in mechanistic terms extends beyond the design procedure of a simple thickness ratio (*10*). This problem is particularly evident in the consideration of stresses and strains leading to the development of punchout distress in CRC pavements. Since it is not reasonable to determine CRC design thickness based on jointed concrete behavior, a constant thickness ratio may not provide adequate reliability against the development of premature punchout distress. Based on a review (*16*) of the nature of and factors leading to punchout distress, a brief discussion and analysis of the failure modes associated with the punchout process in CRC pavements are presented.

BASIC FAILURE MODES LEADING TO PUNCHOUT DISTRESS

Four failure modes, relating to punchout distress based on the results of an in-depth field study (*16*), are proposed as fundamental thickness design considerations for CRC pavements. The analysis of the failure modes is based a priori on uniform support conditions. This analysis requires the use of a non- or low-erodible subbase. The failure modes are illustrated in Figure 1 in typical developmental sequence. Mode I failure is fracturing because of reinforcing bar pullout from the surrounding concrete. Fracturing of this nature has been noted in concrete pullout tests (*17,18*) and develops in the concrete at a steel stress range of 14 to 18 ksi. Field measurements of steel strains at the crack face indicate that this range of stress is frequently exceeded in the colder months of the year. Cyclic bond stresses in the concrete induced from environmental factors can result in a crack growth process, noted in the field study (*16*), around the reinforcing bar, effectively destroying the load transfer capability of the bar as a void develops. Additionally, a loss of bond stiffness (*19*) and pavement bending stiffness occurs. Bearing failure or rebar looseness can also lead to a void around the reinforcement and can have a detrimental effect on the pavement performance similar to the pullout fracture. Pullout failure may be difficult to avoid since the threshold stress is frequently exceeded. Therefore, the load transfer contribution of the reinforcing bar should be ignored.

Mode II, spalling of the transverse crack, is a function of the pavement stiffness. Because of the above assumption about the development of rebar voids, the pavement stiffness is significantly reduced. A certain amount of support loss can be allowed because results from the field study indicate that good performing CRC pavements have experienced some loss of edge support. As suggested in one study, there may be a reduction in pavement stiffness at the cracks because of gradual joint deterioration and declining load transfer efficiency (*20*). These conditions provide adequate justification to determine spall-related stresses based on a reduced pavement stiffness. The pavement stiffness cycles between high and low, mostly as a function of the temperature and the concomitant opening and closing of the cracks. The reduction in stiffness behavior, which occurs on a daily basis, can be assumed to predominate during the winter season. Reduced pavement stiffness is not only a function of the crack width (*21*) but also of the position of the reinforcing steel (*22*). Therefore, spall-related stresses can be determined as a function of the pavement stiffness, design crack width, steel percentage, and the position of the reinforcement in the slab. The narrower the transverse cracks the stiffer the overall pavement system, which in turn lowers the spall-related stresses. This mode of failure is a visual sign of progressive punchout development.

Failure mode III, shown in Figure 1, is a loss of load transfer along transverse cracks. Since the bar is assumed to provide no load transfer, the load transfer of the crack is solely a function of the crack width. Given a constant crack width, the load transfer will decrease under repetitive loading. The resulting load transfer efficiency is based on test results by the Portland Cement Association (PCA) (*5*) for 1 million load applications, which are interpreted as 1 million coverages.

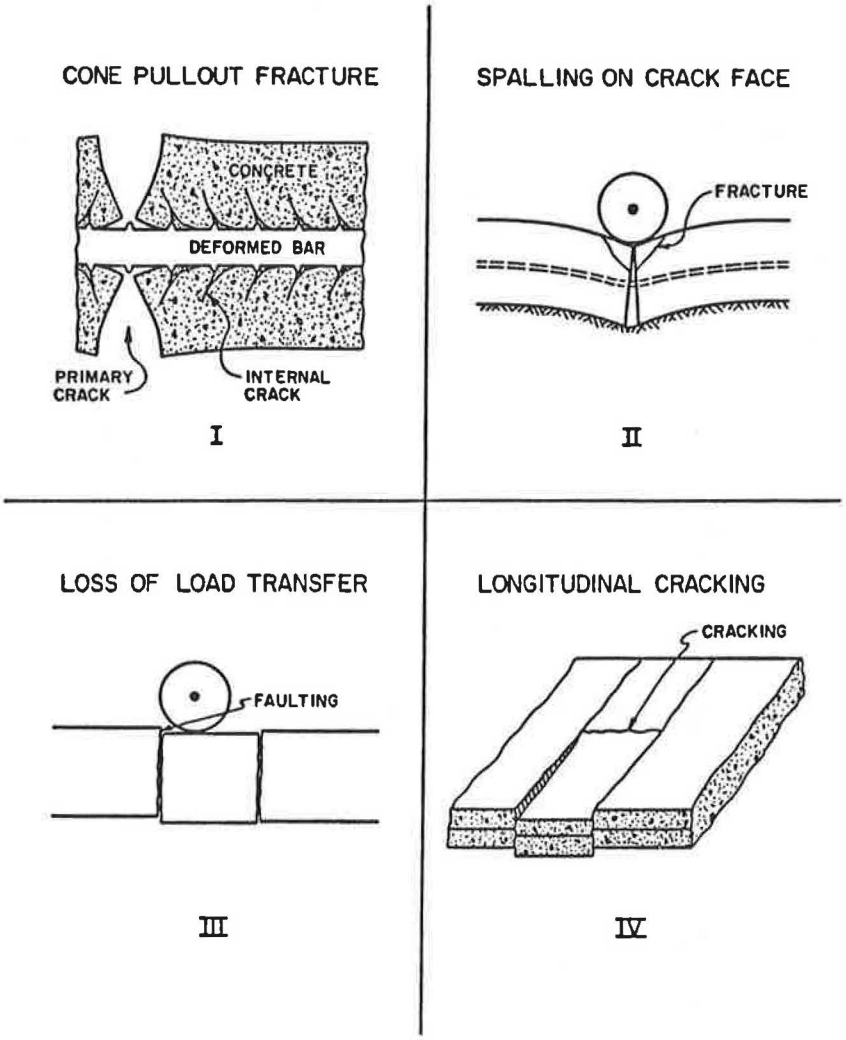

FIGURE 1 Failure modes related to punchout distress in CRC pavement.

The final mode of failure, mode IV, is related to bending stresses in the transverse direction. These stresses typically are not significant in CRC pavement so long as there is a high load transfer across the cracks (before spalling) or the crack spacing is greater than 4 ft. Transverse bending stresses should be considered in most instances since the crack spacing distribution in CRC pavement typically ranges below 4 ft. The load transfer has been noted to decrease significantly with spalling (type 2) in CRC pavements with thicknesses between 8 and 10 in. The transverse bending stresses should be increased in response to the change in load transfer.

SHEAR AND LOAD TRANSFER MECHANISM

As suggested in the description of mode I failure, a reduction in pavement stiffness may result from either pullout failure or bearing failure around the steel, both of which have been observed in field studies. The alternative to the development of excessive bar looseness is cone pullout fracture, which, if it occurs, will be the dominant cause for loss of pavement stiffness. In either case, the load transfer capability of the steel is lost and the load transfer consequently becomes dependent on the crack width and the aggregate interlock. Colley and Humphrey (*5*) of the PCA developed laboratory test data investigating the effect of crack width caused by aggregate interlock on load transfer characteristics in concrete pavements. This study was conducted using an instrumented test slab shown in Figure 2 subjected to a repetitive 9-kip load. The joint in the test slab was an induced crack from a metal strip 1 in. in height placed at the pavement bottom and top. During the repetitive loading, measurements of joint opening and slab deflections on the loaded and unloaded slab were made at regular intervals. The loading sequence across the joint was similar to a continuous application of truck loads traveling approximately 30 mph. Test results in the form of joint effectiveness (E_j), joint opening, and loading cycles for a 7- and a 9-in. slab thickness using a 6-in. gravel subbase are shown in Figure 3*a* and *b*. Joint effectiveness is similar to load transfer efficiency in that if the deflections on the loaded and unloaded slabs are equal then the joint effectiveness is 100 percent. [Note: the load transfer efficiency (LTE) is the unloaded deflection divided by the loaded deflection, in percent.]

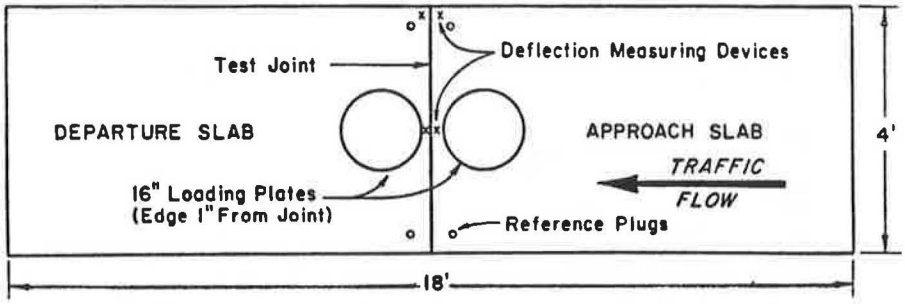

FIGURE 2 Plan of PCA test slab and instrumentation (*5*).

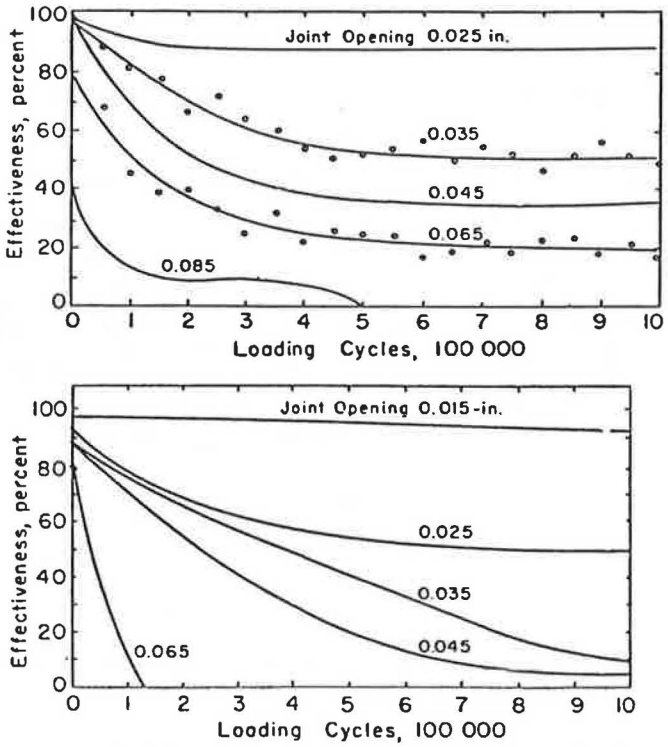

FIGURE 3 Influence of joint opening on effectiveness: (*top*) 9-in. concrete slab, 6-in. gravel subbase (*5*); (*bottom*) 7-in. concrete slab, 6-in. gravel subbase (*5*).

The results indicate that the joint effectiveness tends to level off after about 700,000 to 800,000 load applications. The level of joint effectiveness at 1 million applications may provide a useful basis relating joint or crack width to an ultimate joint effectiveness for design purposes. Figure 4 shows the change in the final joint effectiveness with the joint opening for the 7- and 9-in. thicknesses. Some results were also obtained for other subbase types and are shown in Figure 4, which indicate that foundation strength can improve the load transfer performance. The results from the 7- and 9-in. thicknesses are linearly extended to include other thicknesses. The joint effectiveness from the linear extensions was converted into load transfer efficiency and replotted in Figure 5. Further laboratory tests and field studies should be conducted to validate the extrapolations made from the PCA test data.

To extend the results of the PCA load tests to other load conditions and pavement configurations, load or shear stresses caused by the aggregate interlock must be determined for the test conditions. Using the load results directly is not reasonable since the laboratory loading conditions are different from those in actual CRC pavement. This difference is mostly because of the width of the test specimen, load position, and the height of the roughened interface where the aggregate interlock functioned. All of these factors can be accounted for in the slab analysis model ILLI-SLAB (*13*). This model allows determination of the load transferred by the aggregate interlock at each node along the transverse crack. Modeling the test slab with the ILLI-SLAB program yielded load stresses on the joint face for the test thicknesses plus the range of thicknesses in which the load transfer data had been extended. These results are shown in Figure 6.

Shear stresses can be found from other slab configurations, such as CRC pavement with closely spaced cracking (Figure 7), and related to the test slab conditions. A comparison of

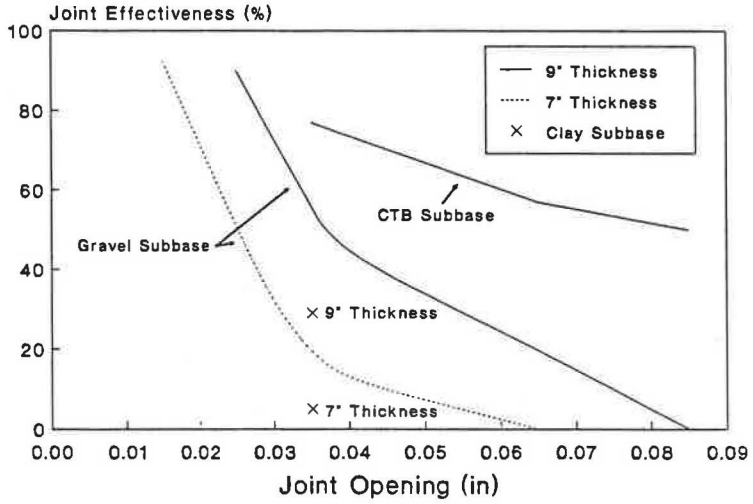

FIGURE 4 Joint effectiveness and joint opening relationship for 1 million load applications.

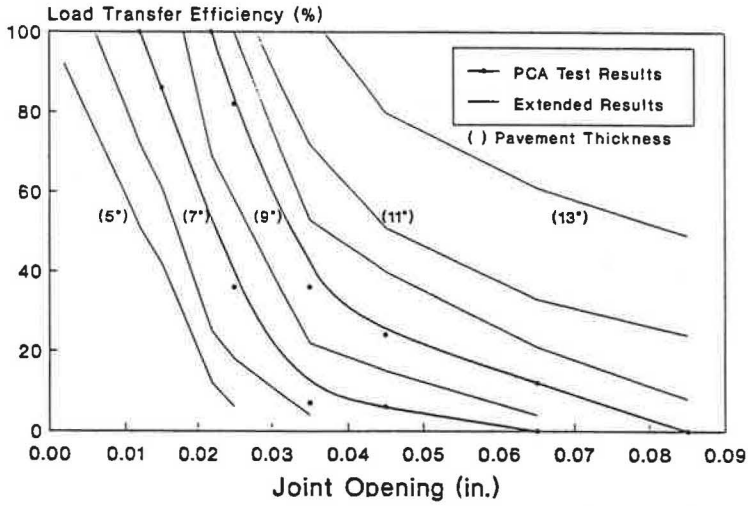

FIGURE 5 Load transfer efficiency and joint opening relationship for thicknesses 5 to 13 in.

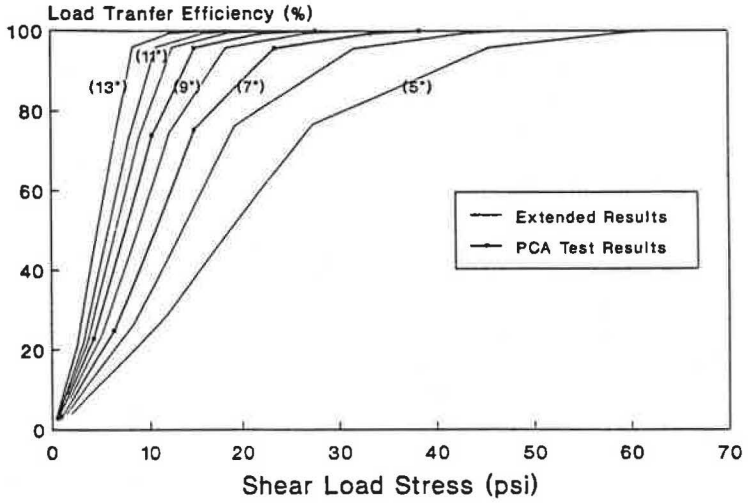

FIGURE 6 Computed load stress for PCA load transfer test results.

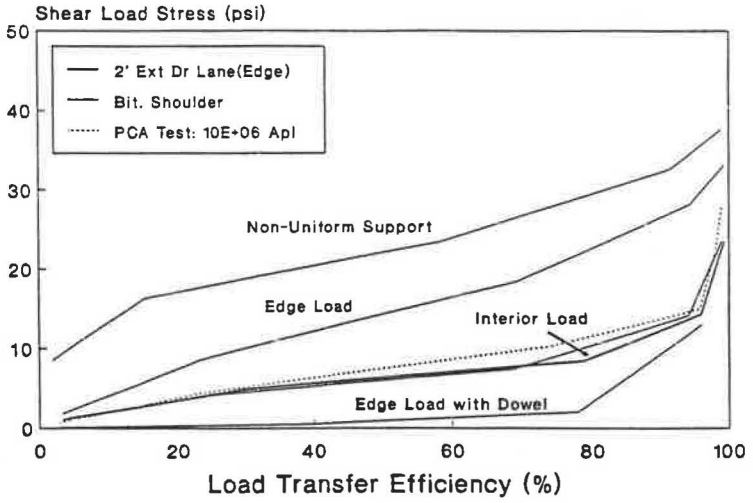

FIGURE 7 Shear load for various load conditions.

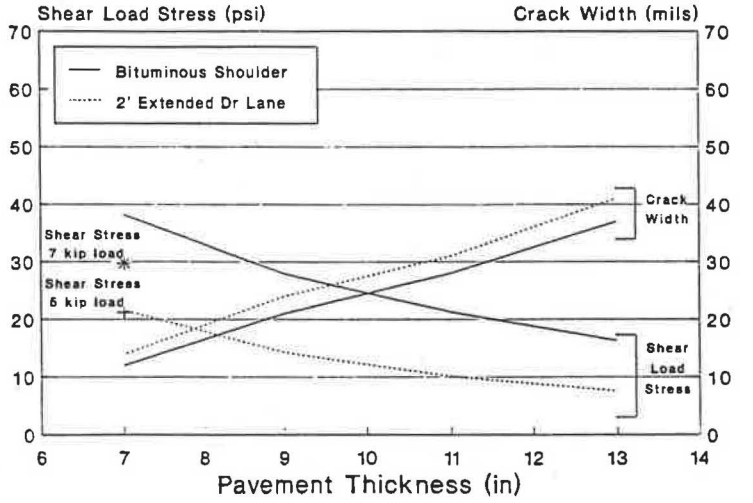

FIGURE 8 Effect of pavement thickness on shear load stress and required crack width (9-kip edge load).

a bituminous shoulder and a 2-ft extended driving lane is made in Figure 7 with the PCA test slab. An edge load position for the bituminous shoulder is adjacent to the outer pavement edge where an edge load position for the extended driving lane is 2 ft from the outer pavement edge. Greater shear stresses occur with a bituminous shoulder condition. The edge loading of a bituminous shoulder with non-uniform support represents the most severe loading conditions for shear stresses, as would be expected. The non-uniform support condition (see Figure 13) extends across the lane under the loaded slab in the ILLI-SLAB model. The loading condition for a 2-ft extended driving lane is not as severe as the loading conditions for the PCA test slab, whereas a bituminous shoulder load condition with the rebar contributing to the load transfer further lowers the shear stress. However, the latter difference is not as pronounced with LTEs greater than 90 percent. Little difference in shear stress is noted between an interior load position (inner wheel path) and the edge load position with the extended driving lane. Similar results were found between a 10-foot tied concrete shoulder and the extended driving lane.

Figure 6 indicates the LTE for a given thickness and load stress information that is entered into Figure 5 to determine the required joint opening (or crack width in the case of CRC pavements) to maintain the given level of LTE for 1 million coverages. Using Figures 6 and 5, in that order, the corresponding limiting crack widths are found and illustrated in Figure 8. This figure draws a comparison of edge loading between a bituminous shoulder and a 2-ft extended driving lane, with change in slab thickness at approximately a 95 percent LTE. This figure describes a fundamental relationship between required or limiting crack width and pavement thickness in terms of load transfer applicable to CRC thickness design.

SPALLING ON THE TRANSVERSE CRACK

Spalling in CRC pavements has been shown to be related to the loss of bending stiffness at the transverse crack (*16*). Discussions and results indicated that the reduction in bending

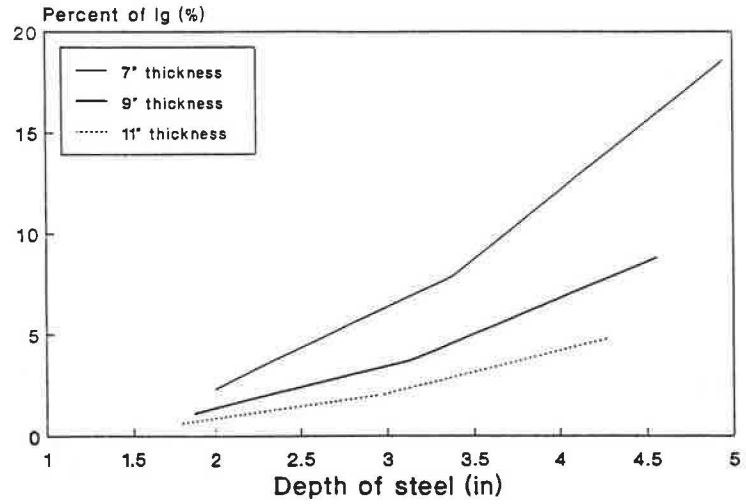

FIGURE 9 Pavement stiffness (I_{crk}) based on percentage reduction of gross moment of inertia (I_g).

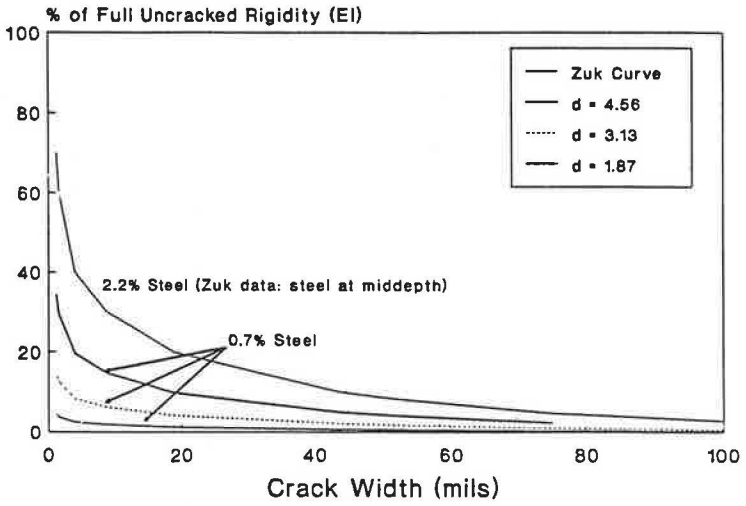

FIGURE 10 Reduction in bending stiffness as a function of crack width (depth of steel noted).

stiffness was cyclic in nature and dependent on the overall pavement temperature. Effective stiffness determined from NDT results indicated that a reduction in pavement bending stiffness of 90 percent was not uncommon. On this basis, spall stress can be determined using equations derived from elastic analysis of a crack section presented for the reduced moment of inertia (I_{crk}):

$$I_{crk} = b(kd)^3/3 + Na_s(d - kd)^2$$

$$= (kd)^3/3 + ntp(d - kd)^2 \text{ (per width } b)$$

where

b = unit width,
kd = distance to the neutral bending axis of the transformed section,
n = modular ratio [steel modulus (E_s)/concrete modulus (E_c)],
d = depth of steel,
t = pavement thickness, and
p = percent of steel [steel area (A_s)/concrete area (A_c)].

The reduced bending stiffness is found from a ratio of the cracked moment of inertia to the uncracked moment of inertia (Figure 9).

Zuk's (*21*) laboratory results for a cracked section shown in Figure 10 provide a relationship between the bending stiffness and the crack width for a cracked section. This relationship is extended to other cracked sections on the basis of the cracked moment of inertia, which is a function of the percent and position of the reinforcement. The percent reinforcement in the test specimens used by Zuk was 2.2 percent. The cracked moment of inertia for the test specimens was 17.9 percent of the gross moment of inertia (I_g). The same analysis can be applied to different thicknesses of CRC pavement shown in Figure 9 for 0.7 percent steel with various depths to the centroid of the reinforcement. Using the ratio between the per-

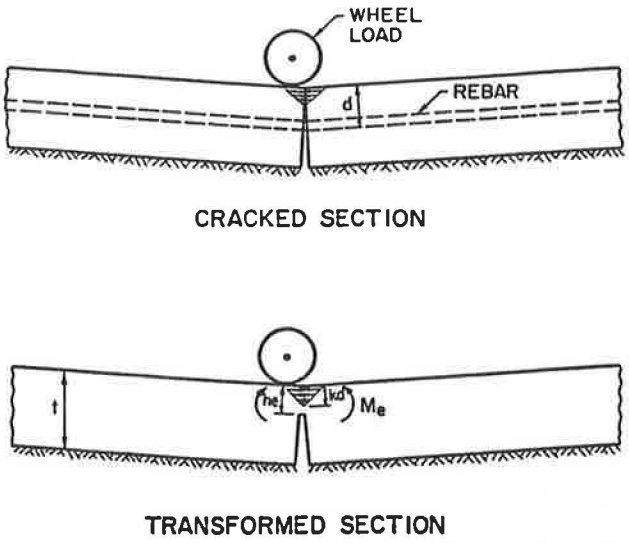

FIGURE 11 Transformation of cracked CRC pavement section.

cent reduction in the I_g for the CRC pavement sections to the percent reduction in I_g of the Zuk test specimens, a bending stiffness and crack width relationship can be developed for CRC pavement shown in Figure 10. In this figure, a comparison between the bending stiffness of a Zuk test specimen and a 9-in. cracked CRC section with 0.7 percent steel placed at various depths is shown. A crack width/stiffness relationship is defined as a function of the depth of steel.

The spall stresses may be found from the compressive and shear stress that develop on the transverse crack face while under load. Shear stresses, which have been discussed previously, and compressive stresses found independently and superimposed on the crack face can be one method of finding the spalling stress. The compressive stresses can be determined using ILLI-SLAB to model a transformed section of CRC pavement. The transformed section is the equivalent of a cracked section with steel reinforcement that has homogeneous material properties and provides the same bending stiffness as the cracked section (Figure 11). The cracked moment of inertia is used to determine the depth (h_e) of the transformed section as $h_e = \sqrt[3]{(12I_{crk})}$ (per unit width). A comparison between the depth to steel (d), depth to the neutral axis (kd), and the equivalent depth (h_e) indicates that the equivalent depth is greater than kd but less than d. The equation for k is found in terms of the depth to the centroid of the steel.

$$k = \{[pn(pn + 2r)]^{1/2} - np\}/r$$

where r is the ratio of the depth to the centroid of the steel (d) to the pavement thickness (t).

The equivalent depth (Figure 11) is input into ILLI-SLAB as the depth of the elements comprising a special case transverse crack. Load transfer by aggregate interlock is normally modeled in the ILLI-SLAB program by a spring element with 1 degree of freedom with displacement in the vertical direction at each node (*13*). The special case transverse crack is represented with reduced depth elements to model the change in bending stiffness that occurs at the crack. Modeling the transverse crack in this manner allows compressive stresses (σ_{ex}) and the bending moment (M_e) to be determined for the equivalent section as

$$M_e = (h_e)^2\sigma_{ex}/6$$

The compressive stress (σ_{cx}) of the cracked section is based on the equivalent bending moment (Figure 12):

$$M_e = Cjd = Tjd$$

$$= \sigma_{cx}kd(d - kd/3)/2$$

$$\sigma_{cx} = 6M_e/[kd^2(3 - k)]$$

The compressive stress is a function of the depth of the reinforcement (d) below the pavement surface, as shown in Figure 13. Compressive stresses for supported and unsupported conditions are included in the figure. In an unsupported condition, the pavement is only partially supported across the width of the lane shown in the figure. This condition is represented in ILLI-SLAB by a reduced K value under the loaded slab. The depth of steel is extended to the bottom of the pavement section, which represents the stresses, which are small, in an uncracked section. The compressive stresses approach this condition for high radius of relative stiffness (l_k) values. (Note: $l_k = [Eh^3/[12\ (1 - \mu)^2k]\}^{1/2}$, where E, h, and μ are the modulus of elasticity, pavement thickness, and Poisson's ratio, respectively.) The compressive stresses are much greater in the region of low l_k values. The compressive stresses are a function of the depth of steel in this region.

The finite element method (FEM) was again employed to develop spall-related stresses from a combined loading of compressive and shear stresses. The FEM mesh with the superimposed loading is shown in Figure 14 in which a 6-in. section of pavement was modeled using a linear, plane strain element. A boundary condition of zero displacement was used on the opposite boundary. The FEM results were consistent as long as the model section of pavement was 6 in. or greater. The maximum tensile stress normally occurs near the neutral bending axis on the crack face. Field results indicated that severe spalling is approximately 2 to 3 in. in depth. Spalling can begin closer to the pavement surface for unsupported conditions since the shear stress may not act over the full pavement thickness. Shear stresses were limited to the pavement above the steel for the unsupported conditions, whereas shear stresses were applied over the full pavement depth for the supported conditions. The support conditions have a sig-

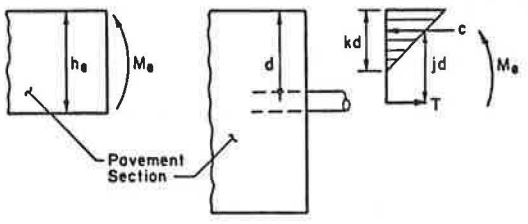

FIGURE 12 Bending moment in equivalent and cracked sections.

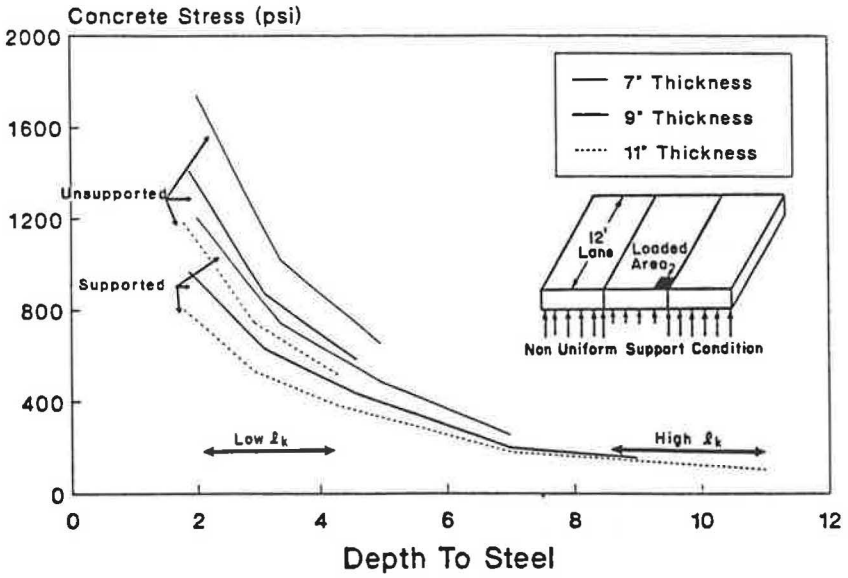

FIGURE 13 Compressive stress for a bituminous shoulder of a cracked section based on ILLI-SLAB analysis.

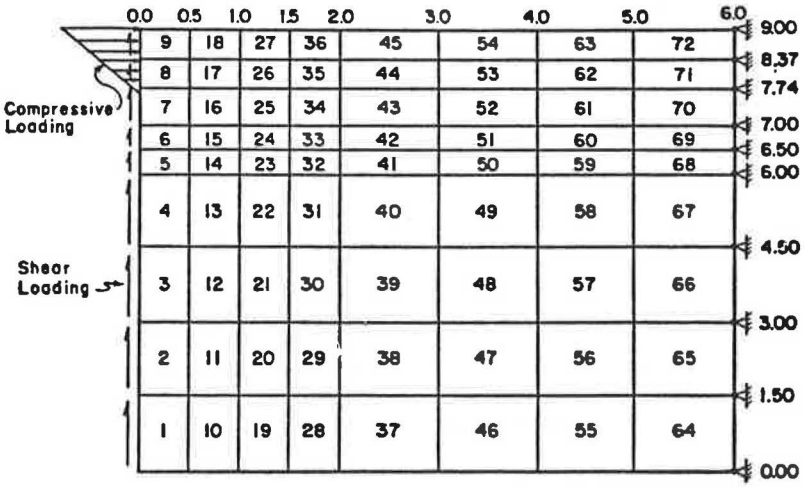

FIGURE 14 Nodal and loading layout for FEM modeling. (Element numbers are shown; nodal coordinates are in inches.)

nificant effect on the spalling stresses. The modeling of unsupported loading conditions tends to verify the field observations. The maximum tensile stresses are shown in Figure 15 as a function of the depth to steel and the support condition. The extended driving lane and the 10-ft tied shoulder reduce spalling stresses approximately 30 percent.

Figures 10 and 15 indicate that the crack width and the depth of steel have an influence on the pavement stiffness and consequently will also influence the spall stresses. Figure 16*a* illustrates the relationship between spall stress and pavement stiffness (caused by the effect of depth of steel). This information can be combined with information from Figure 10 to draw a relationship between crack width and spall stress for a given depth of steel shown in Figure 16*b*. The change in spall stresses is on the order of 50 to 60 psi between the range of crack widths of 10 to 40 mils (1 mil = 10^{-3} in.). Crack widths below 10 mils correspond to low spall stresses. This value corresponds to conditions of high pavement stiffness, as measured by l_k values at transverse cracks approximately 30 in. and greater, which may exist roughly 25 percent of the time.

TRANSVERSE BENDING STRESSES

The formation of longitudinal cracking by lateral stresses caused by wheel load has been thoroughly reviewed by others (*11*). Crack spacing and load transfer have been shown to significantly affect the lateral stresses. Transverse bending stresses (σ_a), illustrated in Figure 17*a*, are low at high values of LTE. Based on ILLI-SLAB results, the effect of support conditions are shown for a 2-ft crack spacing in Figure 17*b*. These stresses are significant below an LTE of 70 percent but increase at a

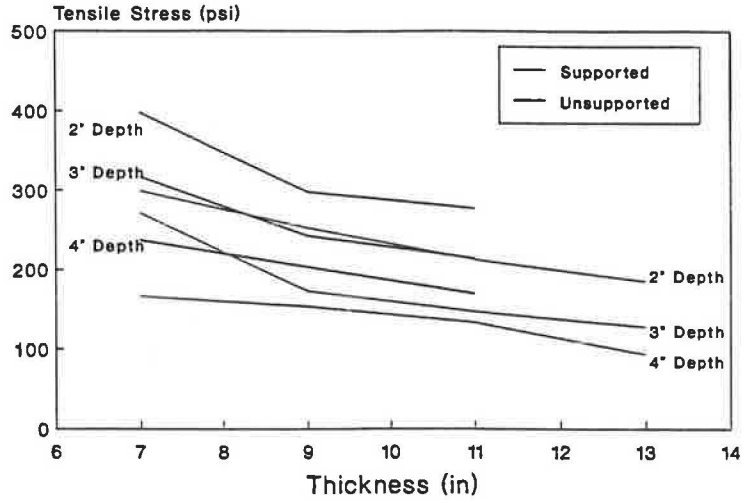

FIGURE 15 Maximum tensile spall stresses for bituminous shoulder.

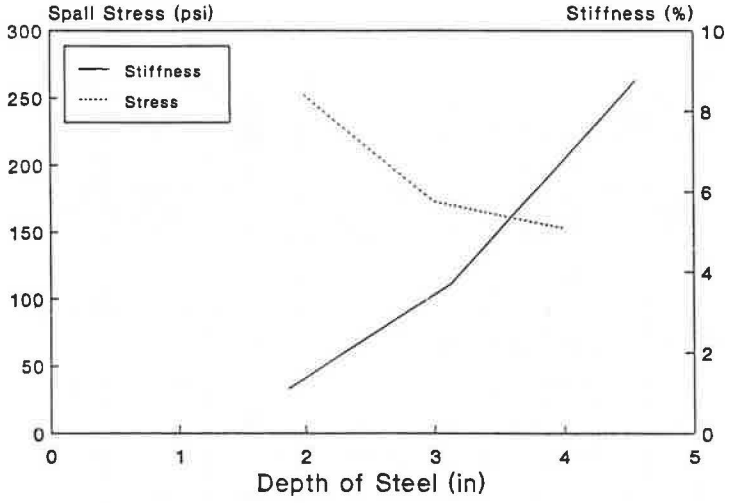

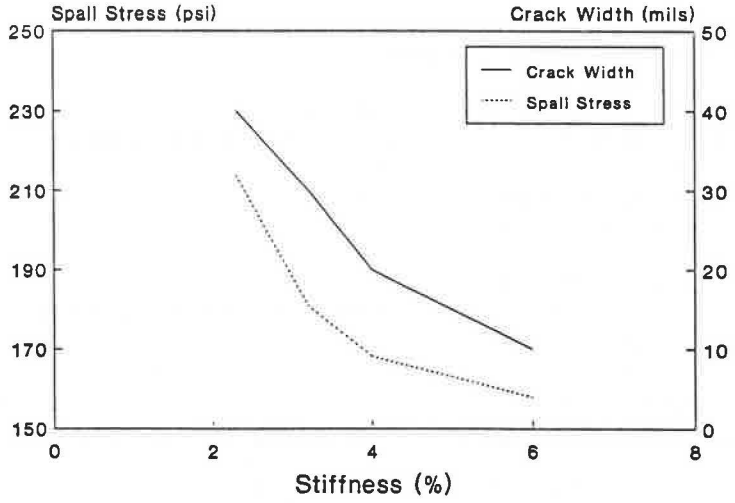

FIGURE 16 (*Top*) Spall stress/stiffness relationship for 9-in. CRC pavement with 0.7 percent steel. (*Bottom*) Spall stress/crack width relationship for 9-in. CRC pavement with 0.7 percent steel (d = 3.1 in.).

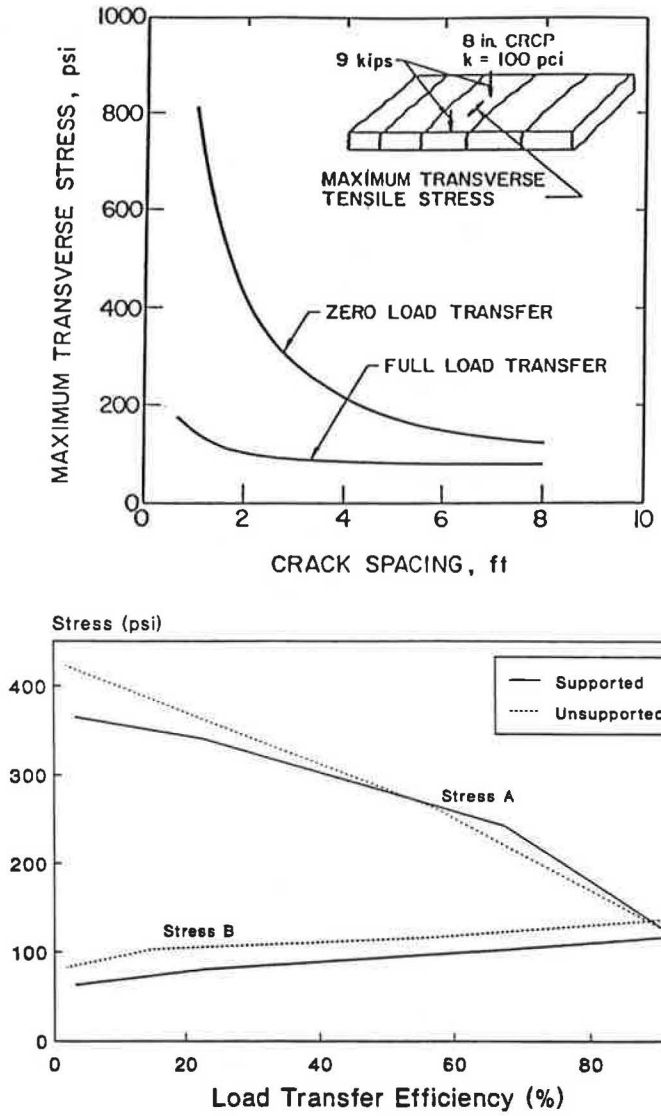

FIGURE 17 (*Top*) **Effect of load transfer across transverse cracks and crack spacing on maximum transverse tensile stress in CRC pavement (*1*).** (*Bottom*) **Transverse and longitudinal bending stresses for 9-in. CRC pavement as a function of LTE (2-ft crack spacing).**

uniform rate below 90 percent LTE. In comparison, the longitudinal bending stresses (σ_b) are relatively low and normally of no concern. According to these results, loss of load transfer has a more significant effect on the bending stresses than does loss of support. The loss of load transfer must develop before longitudinal cracking stresses develop. This point reemphasizes the importance of the spalling mechanism discussed previously in a thickness design procedure.

Figure 18 illustrates a comparison between σ_a and σ_b and provides some basis for selection of optimal crack spacing. The σ_b stress drops with decreasing crack spacing as long as the load transfer remains high. In the case of spalling and loss of load transfer, a crack spacing between 3 and 4 ft is desired. This cracking interval is selected because if the LTE remains high then either of the stresses within that range is not excessive. However, if the LTE becomes low then the stresses corresponding to the high load transfer condition will not be exceeded. Crack spacing outside of this range will cause higher stresses in either case of LTE, leading to a shorter fatigue life. The crack spacing range of 3 to 4 ft provides a balance between the maximum stresses σ_a and σ_b, causing the stresses to be somewhat independent of the load transfer. Spall stresses can have a significant influence on the thickness design for a 2-ft crack spacing but would have less of an impact for a 4-ft crack spacing. Deflection and subgrade stresses are not a problem unless the cracking spacing drops below 3 ft. A balanced condition between stresses σ_a and σ_b results in the case of a 2-ft extended driving lane or a 10-ft tied shoulder for a crack spacing range between 5 and 6 ft. The stresses are much lower than those for the bituminous shoulder case in the 3- to 4-ft range. The stresses in the 3- to 4-ft range for the 2-ft extended shoulder case are approximately 5 to 6 percent lower than the stresses for the bituminous shoulder case in the same range.

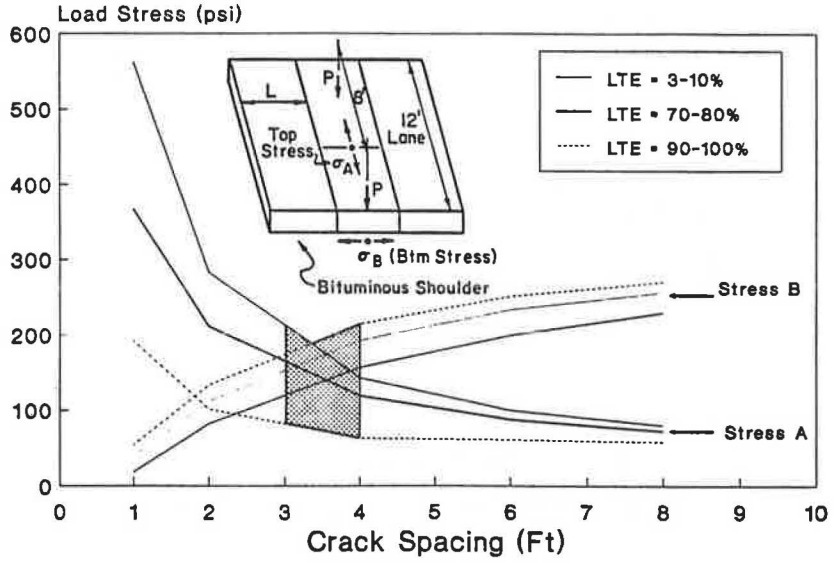

FIGURE 18 Comparison of σ_a and σ_b with crack spacing for a 10-in. pavement thickness.

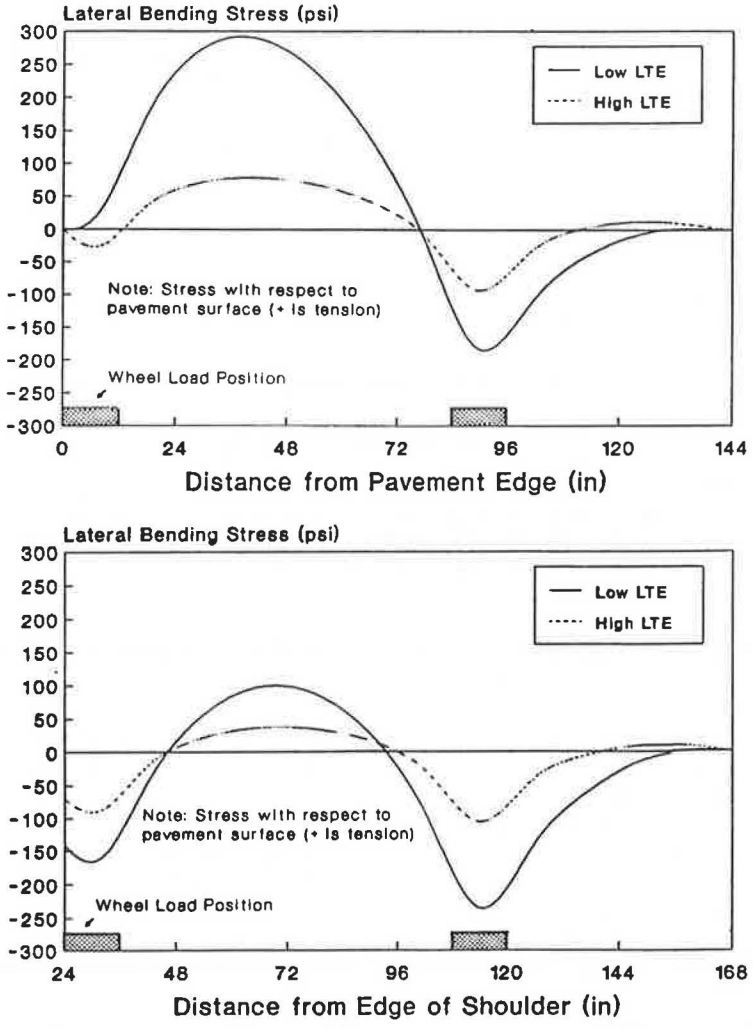

FIGURE 19 Comparison between shoulder types of stress distribution for 9-in. pavement (2-ft crack spacing): (*top*) bituminous shoulder; (*bottom*) 2-ft extended driving lane.

The location of the maximum bending stress is between the wheel load positions approximately 30 in. from the pavement edge for a bituminous shoulder type. The maximum stress location of the 2-ft extended driving lane changes to the inner load position. The stress distribution for these two shoulder types is illustrated in Figure 19 for a 9-in. CRC pavement and for two levels of load transfer. The load behavior for a 10-ft tied shoulder is similar to that for a 2-ft extended driving lane, except that the maximum stresses with a 10-ft tied shoulder are 20 to 30 psi lower.

SUMMARY

Current thickness design procedures inadequately address punchout distress and mechanisms related to it. CRC pavement behavior is different from jointed concrete behavior, and thickness design should not be based on jointed concrete thickness design methods. Design methods that allow for subbase erosion should be based on failure mechanisms leading to punchout distress. CRC pavement performance has indicated that a small amount of erosion can be tolerated, but good design practice should require low or nonerodible subbases. Subbase design is critical to CRC pavement performance since loss of support leading to loss of load transfer has been identified as the primary cause of punchout distress. An optimum crack spacing between 3 and 4 ft is desirable since the maximum longitudinal and transverse bending stresses are minimized in terms of load transfer within this cracking range. Maintaining high load transfer is critical to good CRC pavement performance, particularly outside of this cracking interval, and is highly dependent on the crack width.

Basic failure modes leading to punchout distress were proposed based on a field study and literature surveys of CRC pavement performance. Failure mechanisms were suggested and analyzed in terms of crack widths, pavement stiffness, and load transfer. Although the analysis in some instances extended beyond the limits of the original test data, a useful method was established in which to consider such data and a basis was provided for conducting further testing.

ACKNOWLEDGMENT

This paper is based on the results of a cooperative study between the Illinois Department of Transportation (DOT) and the University of Illinois sponsored by the Division of Highways of the Illinois DOT and FHWA.

REFERENCES

1. W. E. Chastain, Sr., J. A. Beanblossom, and W. E. Chastain, Jr. AASHO Road Test Equations Applied to the Design of Portland Cement Concrete Pavements in Illinois. In *Highway Research Record 90*, HRB, National Research Council, Washington, D.C., Oct. 1965, pp. 26–42.
2. J. S. Dhamrait and R. K. Taylor. *Behavior of Experimental CRC Pavements in Illinois*. Physical Research No. 82. Illinois Department of Transportation, March 1979.
3. "*AASHTO Interim Guide for the Design of Pavement Structures*. AASHTO Committee on Design, AASHTO, Washington, D.C., 1986.
4. *Design of Continuously Reinforced Concrete for Highways*. Associated Reinforcing Bar Producers—CRSI, Chicago, Ill., 1981.
5. B. E. Colley and H. A. Humphrey. *Aggregate Interlock at Joints in Concrete Pavements*. HRB, National Research Council, Washington, D.C., 1967.
6. M. Won and B. F. McCullough. *Research Report 472-2, Texas SDHPT: Evaluation of Proposed Texas SDHPT Design Standards for CRCP*. The Center for Transportation Research, University of Texas, Austin, Dec. 1987.
7. B. F. McCullough, J. C. M. Ma, and C. S. Noble. *Research Report 177-17: Limiting Criteria for The Design of CRCP*. The Center for Transportation Research, University of Texas, Austin, Aug. 1979.
8. J. M. Gregory, A. E. Burks, and V. A. Pink. *Continuously Reinforced Concrete Pavements: A Report of the Study Group*. TRRL Laboratory Report 612. U.K. Transport and Road Research Laboratory, Crowthorne, Berkshire, England, 1974.
9. J. M. Gregory. Continuously Reinforced Concrete Pavements. *Proc. Institution of Civil Engineers*, Part 1, May 1984, 76, pp. 449–472.
10. K. W. Heinrichs, M.-J. Liu, M. I. Darter, S. H. Carpenter, and A. M. Ioannides. *Rigid Pavement Analysis and Design*. Department of Civil Engineering, University of Illinois, Urbana-Champaign, Oct. 1987.
11. S. A. La Coursiere, M. I. Darter, and S. A. Smiley. Performance of Continuously Reinforced Concrete Pavement in Illinois. *Civil Engineering Studies, Transportation Engineering* Series No. 10. University of Illinois, Urbana-Champaign, 1978.
12. *NCHRP Synthesis of Highway Practice 60: Failure and Repair of Continuously Reinforced Concrete Pavement*. TRB, National Research Council, Washington, D.C., July 1979.
13. A. M. Tabatabaie and E. J. Barenberg. Finite-Element Analysis of Jointed or Cracked Concrete Pavements. In *Highway Research Record 671*, HRB, National Research Council, Washington, D.C., 1978.
14. J. Ma, and B. F. McCullough. *Research Report 177-9: CRCP-2, An Improved Computer Program for the Analysis of Continuously Reinforced Concrete Pavements*. The Center for Transportation Research, University of Texas, Austin, August 1977.
15. R. P. Palmer, M. Olsen, and R. L. Lytton. *Research Report 371-2F: TTICRCP—A Mechanistic Model for the Prediction of Stresses, Strains, and Displacements in Continuously Reinforced Concrete Pavements*. Texas Transportation Institute, Texas A&M University, College Station, August 1987.
16. D. G. Zollinger. *Investigation of Punchout Distress of Continuously Reinforced Concrete Pavements*. Ph.D. thesis. University of Illinois, Urbana-Champaign, 1989.
17. D. H. Jiang, S. P. Shah, and A. T. Andonian. Study of the Transfer of Tensile Forces by Bond. *ACI Journal*, Proceedings Vol. 81, No. 3, May–June 1984, pp. 251–259.
18. Y. Goto. Cracks Formed in Concrete Around Deformed Tension Bars. *ACI Journal*, Proceedings Vol. 68, No. 4, April 1971, pp. 244–251.
19. R. M. Mains. Measurement of the Distribution of Tensile Stresses Along Reinforcing Bars. *ACI Journal*, Proceedings Vol. 48, Nov. 1951, pp. 225–252.
20. T. Krauthammer and K. L. Western. Joint Shear Transfer Effects on Pavement Behavior. *Journal of Transportation Engineering*, ASCE, Vol. 114, No. 5, Sept. 1988, pp. 501–529.
21. W. Zuk. Analysis of Special Problems in Continuously Reinforced Concrete Pavements. *Bulletin 214*, HRB, National Research Council, Washington, D.C., 1959.
22. A. Abou-Ayyash and W. R. Hudson. *Report 56-22: Analysis of Bending Stiffness Variation at Cracks in Continuous Pavements*. Center for Highway Research, University of Texas, Austin, August 1975.

Publication of this paper sponsored by Committee on Rigid Pavement Design.